Cent. Eur. J. Phys. • 8(3) • 2010 • 283-288
DOI: 10.2478/s11534-009-0113-x

VERSITA

Central European Journal of **Physics**

Collective mode dispersions of organic chain compounds

Research Article

Željana Bonačić Lošić[1]*, Paško Županović[1]†

University of Split, Faculty of Science, Teslina 12, 21000 Split, Croatia

Received 18 March 2009; accepted 16 June 2009

Abstract: We investigate the collective mode dispersions for the tight-binding dielectric matrix with two one-dimensional electron bands per donor and acceptor chains, and the three-dimensional long-range Coulomb electron-electron interaction within the random phase approximation. The hybridized collective modes are the result of the strong coupling between the intraband plasmon and the interband dipolar modes due to strong dipole Coulomb interactions. Our calculations show the existence of the low-energy renormalized plasmon mode above the electron-hole quasi-continuum in the long wavelength limit. The obtained modes are brought into correspondence with the optical data of quasi-one-dimensional organic conductor tetrathiafulvalene-tetracyanoquinodimethane (TTF-TCNQ). Namely, the renormalized plasmon and the dipolar mode are assigned to the observed excitations at respective energy scales of roughly 10 meV and 0.75 eV, explaining why lower excitation is eliminated while higher excitation persists below the temperature of the Peierls phase transition.

PACS (2008): 71.45.Gm, 77.84.Jd, 78.30.Jw

Keywords: dielectric response • collective modes

1. Introduction

Optical properties of the tetrathiafulvalene (TTF) derivatives are interesting in both non-linear and linear regimes. Most prominently, nonlinear optical materials have attracted a lot of attention lately due to their possible applications in electro-optic devices allowing rapid processing and high density data stocking. The tetrathiafulvalene (TTF) derivatives are of special interest due to the photoinduced nonlinear effects discovered in them [1]. In this paper we are interested in linear optical properties of the tetrathiafulvalene-tetracyanoquinodimethane (TTF-TCNQ), the most intensively studied one-dimensional system.

Early measurements of the optical properties of the quasi-one-dimensional organic conductor TTF-TCNQ [2] have shown a strong angular dependence of excitation at 0.75 eV which is in qualitative agreement with the dispersion of the plasmon mode predicted by Williams and Bloch within the simple model of a quasi-one-dimensional conductor with one one-dimensional electron band per chain in the random phase approximation (RPA) [3]. Further analyses of Williams and Bloch, as well as of Kahn *et al.*, within the extended models [4, 5] with two one-

*E-mail: agicz@pmfst.hr (Corresponding author)
†E-mail: pasko@pmfst.hr

dimensional electron bands, each on a different type of chain, have predicted a second excitation. Williams and Bloch have found that the second coupled plasmon mode has been acoustic, but still both obtained modes have been placed above the electron-hole quasi-continuum in contrast to the experimental findings which did not resolve the two branches [2], whereas Kahn *et al.* have shown that coupling between sublattice plasmons leads to the appearance of the acoustic collective mode in the narrow region between the quasi-continuums of two sublattices where its weak strength makes it unobservable in agreement with experiment.

Also, far-infrared optical measurements have revealed the existence of an optical mode at approximately 10 meV in TTF-TCNQ [6–8]. The frequency of this mode is comparable to the value of the (pseudo) gap Δ_L produced by the $2k_F$ lattice instability at low temperatures ($T < 50$ K), but it cannot be related to this instability since it exists only at high temperatures, where $2k_F$ lattice fluctuations are absent. This is an indication that this mode could be of plasmon origin, but it certainly cannot be understood within a simple plasmon picture [3–5]. On the other hand, the existence of the mode at 0.75 eV even below 50 K, resembles the plasmon excitation in semiconductors at high energy ($\sim 10-20$ eV) [9]. However, closer inspection of the RPA application to the two band insulator (see section 4.5 in reference [9]) shows that so called interband plasmon is coincident with the longitudinal dipolar mode in our approach [10, 11]. Regarding the role of electron-phonon interaction, it is of secondary importance at these energies. Electron-phonon interaction could only screen, *i.e.* renormalize, electron-electron interactions, but this effect wasn't seen in experiments since the measured value of this mode was the same above and below the temperture of phase transition (50 K) [8]. Yet, the elimination of the low-lying mode due to the formation of the insulating gap Δ_L presents the possibility of a mixing of electron-phonon and electron-electron interactions at low temperatures.

As Williams and Bloch have already remarked, the models of Refs. [3–5] do not apply directly to TTF-TCNQ which has bands for which the interband transitions are dipole active (two per each type of molecular chain corresponding to energetically rather close highest occupied molecular orbitals (HOMOs) and lowest unoccupied molecular orbitals (LUMOs) on each TCNQ and TTF site). The lower orbitals participate in the intraband and interband transitions due to partial filling of corresponding bands. Extensive calculations of the stability of TTF-TCNQ show that it is not Madelung energy but dispersive forces, accounted by such orbitals, that stabilize this crystal [11–14]. Thus, motivated by the above questions, in this paper we investigate collective excitations within the model of a quasi-one-dimensional conductor, proposed in Ref. [11], with two dipolar active orbitals per donor and acceptor molecules, *i.e.* two one-dimensional electron bands per each type of molecular chain, with the lower bands being partially filled and the upper empty, and the three-dimensional long-range Coulomb electron-electron interaction. Since the lower orbitals participate simultaneously in both the intraband monopole and interband dipole excitations, we treat monopole-monopole, monopole-dipole, and dipole-dipole Coulomb interactions on an equal footing. It is worthy to note that the role of the Coulomb electron-electron interaction in TTF-TCNQ was recently reinvestigated due to unusual data obtained by angle resolved photoemission spectroscopy (ARPES) [15]. Calculation of the matrix elements in Ref. [15] starts from the charge density of the HOMO of TTF and LUMO of TCNQ. The class of matrix elements calculated in Ref. [15] belong to those which describe electron scattering inside the band *i.e.* they correspond to the on-site, the first, the second, and the third nearest-neighbour contribution to the monopole-monopole interaction. In this work we are interested in the long-wavelength limit and we neglect only on-site contribution to this interaction. In contrast to this local approach we take into account dispersive forces up to the second order in the multipole expansion of Coulomb potential. Our estimation, based on the shift of the excitation energies from 3 eV in pure TCNQ and TTF crystals to 1 eV and less in TTF-TCNQ, shows that particular matrix element of the dipole-dipole potential between nearest neighbouring molecules on the different chains is of the same order of magnitude (1 eV) as the above mentioned numerically calculated matrix element of the local monopole-monople interaction.

2. Analysis and discussion

Applying the recently proposed tight-binding formalism for the dielectric matrix within the random phase approximation (RPA), and proceeding as in Ref. [11], we have determined the energy dispersions of the hybridized collective modes associated with the electron polarization processes. According to the results from Ref. [4] one expects that, at least in the long wavelength limit, four orbitals per primitive cell would lead to four collective excitations above the electron-hole quasi-continuum. However, unlike in Ref. [5] and here, in Ref. [4], electrons have been confined to strands of finite radius and the extent of the localization has had a strong influence on plasmon dispersions. The numerical calculations performed in this paper show that the collective mode with the lowest energy is placed between the acceptor and donor quasi-continuums in the

longwavelength limit in accordance with the predictions based on the numerical calculations within the two-band model used in Ref. [5]. Additionally there are three collective modes above both electron-hole quasi-continuums, the first is a low energy branch that is acoustic in all directions except along the chains, and the other two are optic branches.

Our analysis proceeds by considering the tight-binding dielectric matrix:

$$[\varepsilon] = \begin{bmatrix} 1 - V_{0_a0_a}\Pi_{0_a} & -V_{0_a0_d}\Pi_{0_d} & -V_{0_a1_a}\Pi_{1_a} & -V_{0_a1_d}\Pi_{1_d} \\ -V_{0_d0_a}\Pi_{0_a} & 1 - V_{0_d0_d}\Pi_{0_d} & -V_{0_d1_a}\Pi_{1_a} & -V_{0_d1_d}\Pi_{1_d} \\ -V_{1_a0_a}\Pi_{0_a} & -V_{1_a0_d}\Pi_{0_d} & 1 - V_{1_a1_a}\Pi_{1_a} & -V_{1_a1_d}\Pi_{1_d} \\ -V_{1_d0_a}\Pi_{0_a} & -V_{1_d0_d}\Pi_{0_d} & -V_{1_d1_a}\Pi_{1_a} & 1 - V_{1_d1_d}\Pi_{1_d} \end{bmatrix}, \tag{1}$$

found by Županović *et al.* within the random phase approximation (RPA) [11]. The indices $0_{a(d)} = (0_{a(d)}, 0_{a(d)})$ and $1_{a(d)} = (0_{a(d)}, 1_{a(d)})$ represent intraband and interband one-electron transitions on the acceptor (donor) chains, respectively. The Vs are matrix elements of the bare three-dimensional Coulomb electron-electron interaction, meaning intraband-intraband, intraband-interband, and interband-interband, in the long wavelength limit leading to monopole-monopole, monopole-dipole, and dipole-dipole contributions reading

$$V_{0_e0_f} = \frac{4\pi e^2}{v_0 q^2}, \quad V_{0_e1_f} = \frac{4\pi i e \mu_f q_\parallel}{v_0 q^2}$$

and

$$V_{1_e1_f} = \frac{4\pi\mu_e\mu_f}{3}\left(\frac{3q_\parallel^2}{q^2} - 1\right) + U_{1_e1_f},$$

where $U_{1_e1_f}$ is the short-range part of the Coulomb repulsion, respectively, with the dipole matrix element $\boldsymbol{\mu}_{a(d)}$ oriented along the chain direction $\mathbf{b}$. v_0 is the volume of the unit cell. $\Pi_{0a(d)}$ and $\Pi_{1a(d)}$ are intraband and interband bubble polarization diagrams. After taking into account that the energy gaps on both types of chain $E_{a(d)}$ (≈ 3 eVs) [16] are considerably higher than bandwidths (≈ 0.5 eVs) [17], the interband polarization diagrams reduce to $\Pi_{1a(d)}(\mathbf{q},\omega) = \frac{2n_{a(d)}E_{a(d)}}{\omega^2 - E_{a(d)}^2}$, with the fractional band fillings being $n_{a(d)}$ ($n_d = 2 - n_a$). The intraband polarization diagrams for each type of chains are given by

$$\Pi_{0a(d)}(q_\parallel,\omega) = \frac{4}{N_b}\sum_{k_\parallel=k_F-q_\parallel}^{k_F} \frac{E_{0a(d)}(k_\parallel + q_\parallel) - E_{0a(d)}(k_\parallel)}{\omega^2 - [E_{0a(d)}(k_\parallel + q_\parallel) - E_{0a(d)}(k_\parallel)]^2}, \tag{2}$$

where N_b is the number of the elementary cells along the chains, and k_F is the Fermi wave vector. We consider the tight-binding valence bands $E_{0a}(k_\parallel) = -2t_{0a}(\cos k_\parallel b - \cos k_F b)$ and $E_{0d}(k_\parallel) = 2t_{0d}(\cos k_\parallel b - \cos k_F b)$ for acceptor and donor sublattices, respectively. Here $t_{0a(d)}$ are transfer integrals of valence orbitals along the chains, and the energy is measured from the Fermi energy.

The microscopic dielectric function that corresponds to the determinant of the matrix in Eq. (1) is

$$\varepsilon_m(\mathbf{q},\omega) = \frac{(\omega^2 - \omega_+^2(\mathbf{q}))(\omega^2 - \omega_-^2(\mathbf{q})) - \frac{4\pi e^2}{v_0 q^2}(\Pi_{0a}(q_\parallel,\omega) + \Pi_{0d}(q_\parallel,\omega))(\omega^2 - \omega_{-t}^2)(\omega^2 - \omega_{+t}^2)}{(\omega^2 - E_a^2)(\omega^2 - E_d^2)}. \tag{3}$$

Here

$$\omega_\pm^2(\mathbf{q}) = \frac{1}{2}\left[\omega_a^2(\mathbf{q}) + \omega_d^2(\mathbf{q}) \pm \sqrt{(\omega_a^2(\mathbf{q}) - \omega_d^2(\mathbf{q}))^2 + 16 n_a n_d E_a E_d V_{1_a1_d}^2(\mathbf{q})}\right] \tag{4}$$

are hybrids of interband dipolar modes from two sublattices $\omega_{a(d)}^2(\mathbf{q}) = E_{a(d)}(E_{a(d)} + 2n_{a(d)}V_{1_{a(d)}1_{a(d)}}(\mathbf{q}))$; due to their strong coupling. $\omega_{\pm t}$ denotes the corresponding transverse hybridised dipolar modes ($\mathbf{q} \perp \mathbf{b}$).

The zeroes of microscopic dielectric function (3) determine the energies of the dressed electron-hole excitations. There are two types of dressed electron-hole excitations, namely, incoherent and collective. The difference between the energies of dressed incoherent excitation and its bare electron-hole counterpart with the same wave numbers is of the order of

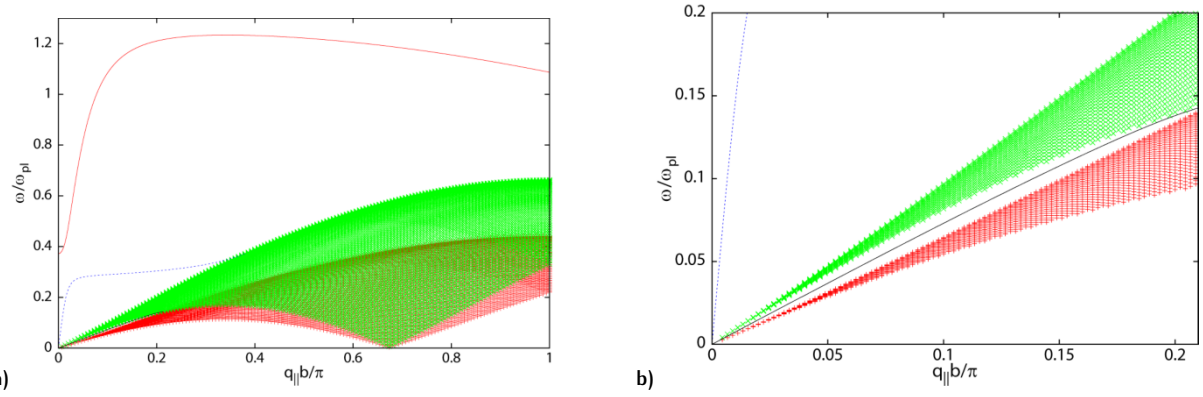

Figure 1. a) Dispersions of the acoustic Ω_1/ω_{pl} (dashed line) and the optic Ω_2/ω_{pl} (solid line) mode for $q_\perp \neq 0$ together with electron-hole quasi-continuum of TTF (lower) and TCNQ (upper) bands and the dispersion of the acoustic mode Ω_4/ω_{pl} in between. Here $\omega_{pl} = \sqrt{\omega_{0a}^2 + \omega_{0d}^2} = 0.9$ eV with $\omega_{0a(d)}$ being longitudinal ($q_\perp = 0$) frequencies of the intraband plasmons $\omega_{0a(d)}^2(\mathbf{q}) = \omega_{0a(d)}^2 q_\parallel^2/q^2$ for the acceptor (donor) sublattice in the longwavelength limit. b) Onset in the longwavelength limit.

$t_{0a(d)}/N_b$. The method for calculating such differences, in the jellium model, is developed in Ref. [18]. On the other hand, there are no a priori limitations on the difference between the energy of collective excitation and the energy of its bare electron-hole counterpart corresponding to the edge of the electron-hole quasi-continuum. This difference depends on the nature of the collective excitation. In the case of intraband/interband excitation (plasmon/Frenkel's exciton) it is of the order of bandwidth/gap. An intraband electron-hole quasi-continuum of a quasi-one-dimensional conductor with two kinds of chains, defined by equations

$$E_{0a(d)}(k_\parallel + q_\parallel) - E_{0a(d)}(k_\parallel) = 4t_{0a(d)} \sin\frac{2k_\parallel + q_\parallel}{2} b \sin\frac{q_\parallel b}{2}, \tag{5}$$

is depicted in Fig. 1. The two differently colored areas refer to the energies of the electron-hole excitations in the acceptor and donor sublattices, respectively.

Here we calculate the energy dispersions of collective modes in the long wavelength limit. Since there are macroscopic differences between the collective excitations and their electron-hole counterparts, one can calculate collective mode dispersions using a standard continuous approximation. Then, the polarisation diagrams in Eq. (2) are

$$\Pi_{0a(d)}\left(q_\parallel, \omega\right) = \frac{2}{\pi}\begin{cases} \frac{1}{\sqrt{\omega^2 - \Delta_{a(d)}^2\left(q_\parallel\right)}}\left[\arctan\frac{\cos\frac{2k_F - q_\parallel}{2} b}{\sqrt{\frac{\omega^2}{\Delta_{a(d)}^2\left(q_\parallel\right)} - 1}} - \arctan\frac{\cos\frac{2k_F + q_\parallel}{2} b}{\sqrt{\frac{\omega^2}{\Delta_{a(d)}^2\left(q_\parallel\right)} - 1}}\right], & \omega > \Delta_{a(d)}\left(q_\parallel\right), \\ \frac{1}{2\sqrt{\Delta_{a(d)}^2\left(q_\parallel\right) - \omega^2}}\left[\ln\left|\frac{\cos\frac{2k_F - q_\parallel}{2} b - \sqrt{1 - \frac{\omega^2}{\Delta_{a(d)}^2\left(q_\parallel\right)}}}{\cos\frac{2k_F - q_\parallel}{2} b + \sqrt{1 - \frac{\omega^2}{\Delta_{a(d)}^2\left(q_\parallel\right)}}}\right| - \ln\left|\frac{\cos\frac{2k_F + q_\parallel}{2} b - \sqrt{1 - \frac{\omega^2}{\Delta_{a(d)}^2\left(q_\parallel\right)}}}{\cos\frac{2k_F + q_\parallel}{2} b + \sqrt{1 - \frac{\omega^2}{\Delta_{a(d)}^2\left(q_\parallel\right)}}}\right|\right], & \omega < \Delta_{a(d)}\left(q_\parallel\right), \end{cases} \tag{6}$$

where $\Delta_{a(d)}(q_\parallel) = 4t_{0a(d)} \sin\frac{q_\parallel b}{2}$ is the higher edge of the acceptor (donor) electron-hole quasi-continuum. Hence, the results for the collective mode dispersions follow from Eq. (3) after taking the polarization diagrams (6) derived through continuous approximation into account. Therefore, the resulting collective modes, denoted $\Omega_{1,2,3,4}(\mathbf{q})$ below, are the zeroes of the thus obtained dielectric function. Their origin is in the strong coupling between the interband dipolar modes and the intraband plasmons from the two sublattices. Dipolar modes (≈ 3 eV) have higher frequencies then plasmon modes (≈ 1 eV), thus the resulting high and low frequency hybridised modes are, in their origin, dipolar and plasmon modes, respectively.

In particular, we consider the case of the orthorhom-

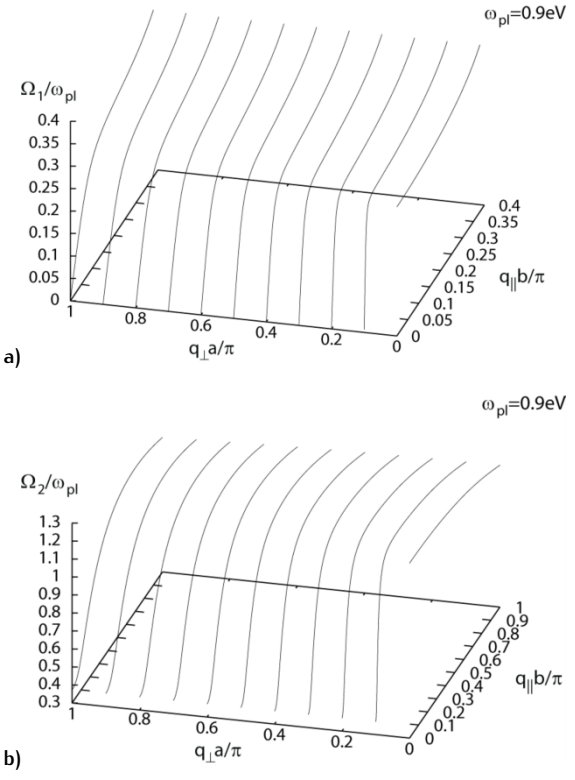

Figure 2. Dispersions of modes $\Omega_1(\mathbf{q})/\omega_{pl}$ (a) and $\Omega_2(\mathbf{q})/\omega_{pl}$ (b) above the electron-hole quasi-continuum from Fig. 1.

bic counterpart of TTF-TCNQ lattice with parameters of $t_{0a} = 0.15$ eV, $t_{0d} = 0.1$ eV, $k_F = 0.132a_0^{-1}$ and $U_{1_a1_d} = 1.52$ eV. The wave vector dependence of the collective mode frequencies are determined numerically. The results for $q_\perp \neq 0$ are depicted in Fig. 1 a). The collective mode Ω_1 is acoustic and becomes an incoherent excitation for $q_\parallel > q_c \approx 0.4\pi/b$, while the collective mode Ω_2 stays well above the electron-hole quasi-continuum throughout the whole I Brillouin zone. The mode Ω_3, not shown in Fig. 1, is situated at the frequencies of a few eVs that were not experimentally investigated in detail. As shown in Fig. 2, modes Ω_1 and Ω_2 are strongly anisotropic in the long wavelength limit. It can be seen that both modes are optic for $q_\perp = 0$. The dispersion of the mode Ω_1 qualitatively resembles that of the plasmon mode for a single one-dimensional electron band, but quantitatively its energy is considerably reduced due to the strong coupling of dipolar and plasmon modes. Its small value is due to the dominance of U_{1a1d} over U_{1a1a} and U_{1d1d} which are neglected in the calculation to emphasize this point. Namely, Ω_1 is small only if the frequency of the lower transverse hybridised dipolar mode ω_{-t} is small, which is the case provided

$$V_{1_a1_d,t} \approx \frac{\omega_{at}\omega_{dt}}{2\sqrt{n_a n_d E_a E_d}}, \tag{7}$$

as seen from Eq. (4). The transverse dipolar frequencies for two chain sublattices presumably satisfy $\omega_{a(d)t} \approx E_{a(d)}$ [16]. This means $E_{a(d)} \gg V_{1_{a(d)}1_{a(d)}}$ which leads to the requirement $E_a, E_d, V_{1_a1_d} \gg V_{1_a1_a}, V_{1_d1_d}$. Since the product of the long-range parts of $V_{1_a1_a}$ and $V_{1_d1_d}$ is of the same order of magnitude as the square of the long-range part of $V_{1_a1_d}$, the dominance of $V_{1_a1_d}$ is to be found in the short-range contributions from nearest neighbouring pairs of donor and acceptor chains. Only short-range dipole-dipole interaction between nearest neighbour pairs of donor and acceptor molecules (≈ 1.5 eV) is shown to be of importance for the appearance of the low energy collective mode Ω_1. However, quantitatively this interaction has approximately the same value as the short-range monopole-monopole interaction calculated in Ref. [15]. Only intraband transitions contribute to monopole-monopole interaction and splitting of the high temperature valence band, below the Peierls temperature, into low temperature, full valence, and empty conduction subbands, obstructs monopole-monopole contribution to the effective interactions. Namely, as the valence sub-band is full, a polarization diagram for transitions within the valence sub-band vanishes at $T = 0$. Similarly, as the conduction sub-band is empty, a polarization diagram for virtual transition in this sub-band vanishes too. The contribution to the effective interaction comes only from dipolar transitions and the crystal behaves like an insulator below the Peierls temperature. Modes Ω_1 and Ω_2 can be directly associated with the optical data of TTF-TCNQ. Mode Ω_1 can be assigned to the excitation at ≈ 10 meV observed at 100K in the infrared measurements [6–8], while mode Ω_2 corresponds to the excitation at ≈ 0.75 eV [2]. The supporting reasons include the following: The measurements show [6, 8] that the low-lying excitation at ≈ 10 meV disappears below 50 K, which is the temperature of the Peierls transition for TTF-TCNQ. The collective mode Ω_1 is a renormalised intraband plasmon. It does not exist in insulators, meaning a Peierls insulator in this case. Furthermore, the modulation of the crystal structure in the insulating phase below the temperature of the Peierls phase transition also causes a weak splitting of the transverse interband dipolar mode ω_{-t} [11] which is in analogy with the Davydov splitting of molecular excitons [19]. Such splitting is indeed observed for the excitation at ≈ 50 meV in the infrared data of TTF-TCNQ [8] corresponding to mode ω_{-t} [11]. We expect that more refined measurements would show the same splitting for the excitation at 0.75 eV, thus confirming the dipolar origin of mode Ω_2. Furthermore, our results show that the hybridised collective mode

with the lowest energy (Ω_4) is acoustic for all the directions of wave vectors **q**, as shown in Fig. 1 b) for $q_\perp \neq 0$. Mode Ω_4 appears as a collective excitation due to the opening of the gap in the electron-hole quasi-continuum between the lower edge of the acceptor (donor) contribution $\delta_{a(d)}(q_\parallel) = 4t_{0a(d)} \sin \frac{2k_F - q_\parallel}{2} b \sin \frac{q_\parallel b}{2}$ and the higher edge of donor (acceptor) contribution $\Delta_{d(a)}(q_\parallel)$ in the long wavelength limit for the longitudinal wave vectors $q_\parallel$ in the region between 0 and $2k_F - \frac{2}{b} \arcsin \frac{t_{0d}}{t_{0a}}$ if $t_{0d} < t_{0a} \sin k_F b$ (or in the region between 0 and $2k_F - \frac{2}{b} \arcsin \frac{t_{0a}}{t_{0d}}$ if $t_{0a} < t_{0d} \sin k_F b$). The prediction of such a mode is intrinsic to the quasi-one-dimensional case. In the two- or three-dimensional isotropic crystal a low energy gap is not present. Although small interchain hopping $t_\perp$ in a real quasi-one-dimensional conductor, as well as the monoclinic crystal structure of real TTF-TCNQ, could affect the low-energy gap.

To account for the anisotropy, it is conventionally agreed that the effective mass changes with the crystal direction. To quantify the degree of anisotropy it is customary to use the effective-mass ratio in the various directions, $\Gamma_{a(d)} = m^*_{\perp a(d)}/m^*_{\parallel a(d)}$, where $m^*_{\parallel a(d)} = \frac{\hbar^2}{2t_{0a(d)}b^2}$ and $m^*_{\perp a(d)} = \frac{\hbar^2}{2t_{\perp a(d)}c^2}$ are effective masses. In the particular case of TTF-TCNQ acceptor and donor interchain transfer integrals in the transverse c direction between the chains of same type, $t_{\perp a} = 1.7$ meV for TCNQ and $t_{\perp d} = 0.3$ meV TTF chains [20]. In TCNQ sublattice, the effective mass ratio is $\Gamma_a = 1.94$. TTF sublattice exhibits somewhat higher anisotropy, $\Gamma_d = 7.49$.

3. Conclusion

In conclusion, the present analysis shows the existence of the low energy collective mode outside the electron-hole quasi-continuum in the long wavelength limit for the model of a quasi-one-dimensional conductor with four orbitals per primitive cell. Also, the present analysis indicates the importance of the long-range dipole Coulomb electron-electron interaction in the optical properties of TTF-TCNQ. Strong dipole Coulomb interactions leading to strong coupling between intraband plasmon and interband dipolar modes result in hybridized collective modes. These modes explain the low frequency optical data in TTF-TCNQ.

References

[1] B. Sahraoui, I. V. Kityk, P. Hudhomme, A. Gorgues, J. Phys. Chem. B 105, 6295 (2001)

[2] J. J. Ritsko et al., Phys. Rev. Lett. 34, 1330 (1975)

[3] P. F. Williams, A. N. Bloch, Phys. Rev. B 10, 1097 (1974)

[4] P. F. Williams, A. N. Bloch, Phys. Rev. Lett. 36, 64 (1976)

[5] L. M. Khan, J. Ruvalds, Phys. Rev. B 17, 4600 (1978)

[6] D. B. Tanner et al., Phys. Rev. B 13, 3381 (1976)

[7] C. S. Jacobsen, In: S. Barišić et al. (Ed.), Leture Notes in Physics 95, (Springer-Verlag, New York, 1979) 223

[8] H. Basista et al., Phys. Rev. B 42, 4088 (1990)

[9] I. Egri, Phys. Rep. 119, 363 (1985)

[10] P. Županović, A. Bjeliš, S. Barišić, Z. Phys. B 101, 397 (1996)

[11] P. Županović, A. Bjeliš, S. Barišić, Europhys. Lett. 45, 188 (1999)

[12] R. M. Metzger, A. N. Bloch, J. Chem. Phys. 63, 5098 (1975)

[13] A. J. Epstein et al., Phys. Rev. B 13, 1569 (1976)

[14] R. M. Metzger, J. Chem. Phys. 75, 3087 (1981)

[15] L. Cano-Cortés et al., Eur. Phys. J. B 56, 173 (2007)

[16] R. R. Pennelly, C. J. Eckhardt, Chem. Phys. 12, 89 (1976)

[17] D. Jérome, H. J. Schulz, Adv. Phys. 31, 299 (1982)

[18] P. Županović, A. Bjeliš, Ž. Agić, Fizika A (Zagreb) 10, 203 (2001)

[19] A. S. Davydov, Theory of Molecular Excitations (Plenum Press, New York, 1971)

[20] A. J. Berlinsky, J. F. Carolan, L. Weiler, Solid State Comm. 15, 795 (1974)